DOI 10.52209/2706-977X_2024_3_3 **IRSTI 81.09.03** **UDC 620.179.112**

About the Friction Mechanism in Graphite and Diamond

Yurov V.M.[1], Portnov V.S.[2], Zhangozhin K.N.[1], Rakhimova G.M.[2*], Rakhimova Zh.B.[2]

[1]LLP "TSC-Vostok", Karaganda, Astana, Kazakhstan
[2]Abylkas Saginov Karaganda Technical University, Karaganda, Kazakhstan
*corresponding author

Abstract. A model of graphite friction is proposed. In this model, the friction process is described as a process of elastoplastic deformation of the surface layer. Moreover, the nanolayer, which contains 3–5 atomic monolayers, behaves elastically and quickly collapses according to the Griffiths scheme, forming a layer like a solid lubricant. Next, the mesoslayer enters into the friction process. If the friction of graphite is considered similar to the friction of a viscous liquid, then from this approach it follows that friction depends on the speed of movement, has a structure similar to Benard cells, which means self-organization and friction synergism occurs. The fact that the friction of graphite cannot be explained using the usual Amonton law or on the basis of the hydrodynamic theory of lubrication is due to the fact that it is associated with the viscosity of the solution, the theory of which has not yet been completed.

Due to the reconstruction of its surface, the surface layer of metastable diamond becomes graphite and its friction coefficient is the same value k ≈ 0.1. If you remove the surface layer of metastable diamond, i.e. turning it into a diamond, then its friction coefficient will be k ≈ 0.6.

Keywords: graphite, diamond, friction, surface, self-organization, synergetics, speed, lubrication, elasticity.

Introduction

The performance of parts of various moving mechanisms and machines is mainly affected by friction. Currently, there are five theories that explain the processes occurring during friction: mechanical (deformation); molecular (adhesive); molecular mechanical; energy; hydrodynamic [1]. The study of the friction process is over 500 years old [2] and continues to this day, due to the emergence of extreme conditions: high processing speeds of various metal products, high pressures, high temperatures, aggressive environments, etc. [3]. In the theory of friction, it is necessary to take into account both the mesoscopic approach [4] and the nanostructural approach [5]. In [6], a mechanical friction quantum was proposed. During friction, especially under lubrication conditions, as well as in dry friction, it is necessary to take into account the self-organization and synergy of the rubbing materials [7, 8].

In this article, we will review and propose the friction mechanism of two allotropic modifications of carbon - graphite and diamond.

A graphite crystal is a layered structure consisting of graphene layers. Each layer consists of regular hexagons of carbon atoms (C) measuring 0.335 nm, between which there are strong covalent bonds with an energy of 170 J/mol. Between the layers there is a space of 0.7-1.6 nm in size, where weak Van der Waals forces act with an energy of 16.7 J/mol (Fig. 1a). These graphene layers easily slide in the longitudinal direction and represent a solid lubricant (Fig. 1b).

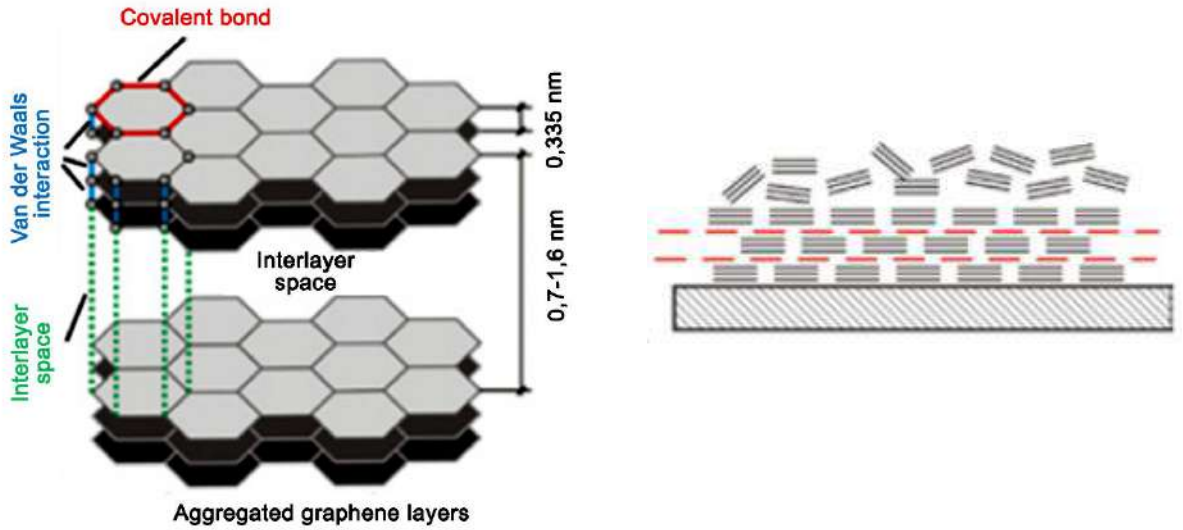

a) b)

Fig. 1. Structure of graphite (a) and layer diagram on the metal (b) [9]

In work [10], graphites of various grades according to GOST [11] were used for solid lubrication. It has been shown that colloidal graphite containing dispersed particles provides the best antifriction properties of metal composite materials. Antifriction graphite and its application in industry have long been used [12]. In Kazakhstan, a monograph is devoted to carbon materials [13].

The coefficient of friction of diamond on metal materials is 0.1, which leads to high abrasion resistance of diamond, which is 90 times greater than the wear resistance of corundum, and 100 and 1000 times greater than that of various abrasive materials. Diamond powders are indispensable for processing parts made of hard alloys [14, 15]. A large amount of information on diamond is available in [16].

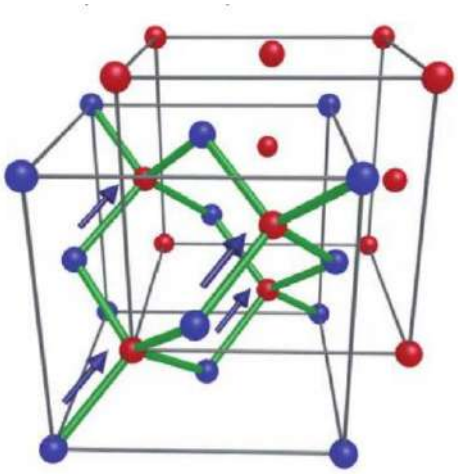

a)

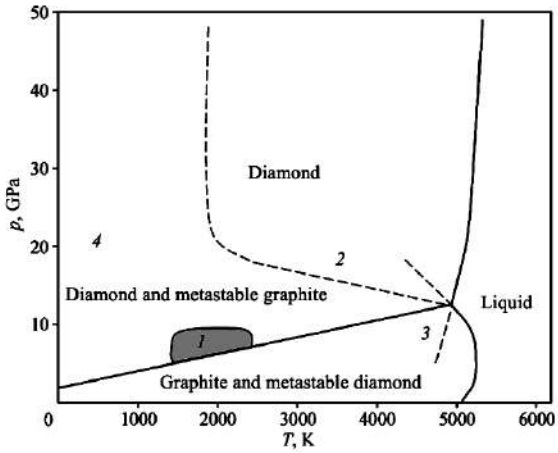

b)

Fig. 2. Diamond lattice (a) [16]; Bundy carbon phase diagram [17]

The structure of diamond consists entirely of carbon (Fig. 2a) and belongs to the Fd3m symmetry. Lattice parameter a = 0.35667 nm, density ρ = 3.52 (g/cm^3), molar mass M = 12.01 (g/mol) [16]. The Bundy phase diagram of carbon is shown in Fig. 2b [17]. In the periodic table of Mendeleev D.I. shows the position of carbon in the central column and top row (Fig. 3a). In the central column, carbon has the most covalent bonds per atom (4). The top position makes its atoms the smallest among all the elements in the central column. The combination of these two attributes gives diamond the highest concentration of binding energy and thereby gives it unmatched hardness and other beneficial properties [18].

In Fig. 3b shows the dependence of the friction coefficient on hardness. As you can see, diamond has a friction coefficient of about 0.1, just like graphite. As a result, diamond powder (DLC) can protect engine parts from further mechanical wear or chemical erosion. In addition, the opposing moving parts now slide on a solid surface that has a coefficient of friction much lower than that of any metal component (Fig. 3b). The movement of the engine part will receive much less resistance and less energy (such as gasoline) needed to power the engine.

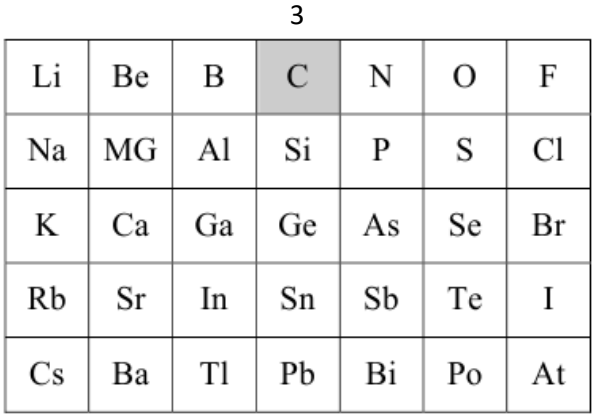

a)

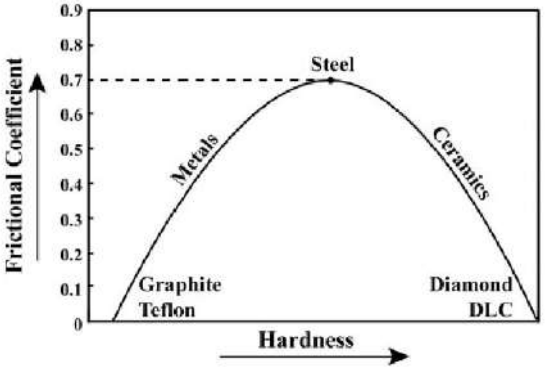

b)

Fig. 3. Periodic table of D.I., showing solid materials with atomic bonds. This table does not include hydrogen and noble gases (a); friction coefficient as a function of hardness (b) [18]

Diamonds and diamond powder are widely used in industry [19], electronics and optics [20]. From Fig. 2b it follows that under ordinary conditions diamond is a metastable structure [17]. It becomes stable at high pressure and high temperature [21, 22] or at sizes less than 30 μm, when it becomes a nanodiamond [23, 24].

1. Research methodology

It has now become generally known that friction is significantly related to the surface layer of a solid [1-3]. Determining the thickness of this layer R(I) experimentally is a very difficult task, requiring ultra-high vacuum and complex equipment [25]. This problem has been solved only for a few substances. For example, for gold R(I) = 1.2 nm, and for silicon - R(I) = 3.2 nm [25], i.e. they are a nanostructure. Theoretically, we first determined the thickness of the surface layer of solids in [26-28] (Fig. 4a), and friction in [29] (Fig. 4b).

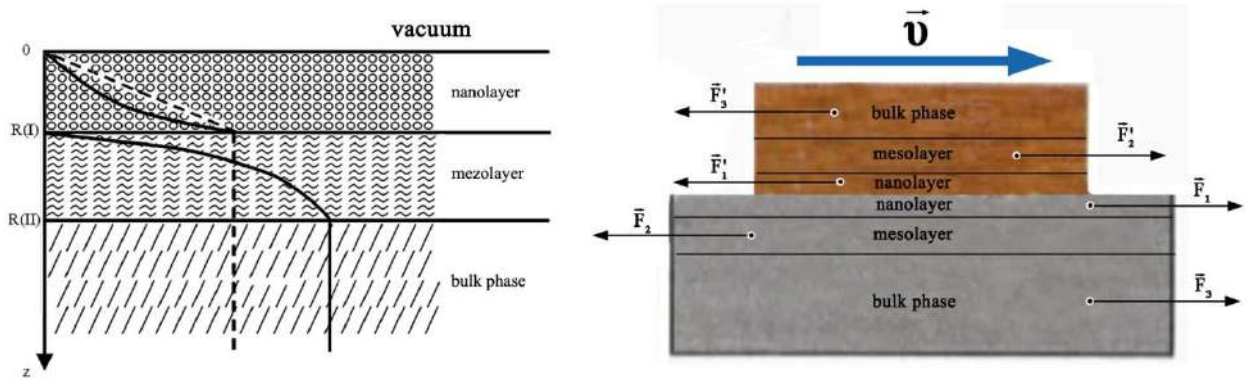

a) b)

Fig. 4. Scheme of a solid: nanolayer → mesolayer → bulk phase [28] (a); diagram of the movement of atomically smooth diamond and graphite on atomically smooth metal surfaces with a constant speed υ [29].

The thickness of the surface layer R(I) is given by the formula [26-28]:

$$R(I) = 0{,}17 \cdot 10^{-9} \cdot \alpha \cdot \upsilon \ [m]. \quad (1)$$

In equation (1), you need to know one parameter - the molar volume of the element, which is equal to υ = M/ρ (M is the molar mass, ρ is its density), α = 1 m^{-2} - a constant, so that the dimension (R(I) [m]). Using formula (1), we calculate R(I) (Table 1) for graphite parallel to the plane x = a = b and perpendicular to this plane x = c [30].

Table 1. Parameters R(I) of graphite.

Graphite	Structure	M, g/mol	ρ, g/sm^3	$R(I)_a$, nm	$R(I)_c$, nm
C	C6/mmc-D^4_{6h}	12,0107	2,26	0.90 (3)	2.46 (3)
			1,75	1.17 (4)	3.19 (4)
			1,65	1.24 (5)	3.39 (5)

From the table It can be seen from Fig. 1 that the thickness of the $R(I)_a$ layer varies from 0.9 to 1.24 nm in the upper plane, and the thickness of the $R(I)_c$ layer varies from 2.46 to 3.39 nm perpendicular to this plane. This is due to changes in the density of graphite and its layered structure. Natural graphite has ρ = 2.26 g/cm^3, and artificial graphite has ρ = (1.75-1.65) g/cm^3. The number of monolayers in graphite is given in parentheses - $n = R(I)_{a,\,c}/a, c$ (a, c are lattice constants). In the R(I) layer, the number of monolayers varies from 3 to 5, depending on the porosity of the graphite. It is shown in [31] that the surface energy of a bulk metal γ_2, with an accuracy of 3%, is equal to:

$$\gamma_2 = 0{,}7 \cdot 10^{-3} \cdot T_m \ [J/m^2], \quad (2)$$

where T_m is the melting temperature of the metal (K).

In the R(I) layer, it is necessary to take into account the size effect and the surface energy of the R(I) layer becomes equal to γ_1 [32]:

$$\gamma_1 = \gamma_2(1 - R(I)/R(I) + h) \approx 0{,}3\gamma_2 , \quad (3)$$

Equation (3) shows that the surface energy of the R(I) layer is three times less than the surface energy of the main crystal. To separate the R(I) layer from the rest of the crystal, it is necessary to expend energy, which is called adhesion energy [32]:

$$W_a = \gamma_1 + \gamma_2 - \gamma_{12} \approx \gamma_1 + \gamma_2 = 1.3\gamma_2, \quad (4)$$

where γ_{12} is the surface energy at the phase interface, which is negligible due to a second-order phase transition.

Internal voltages σis between phases γ_1 and γ_2 can be calculated using the formula [33]:

$$\sigma_{is} = \sqrt{W_a \cdot Å / R(I)}, \quad (5)$$

where E is Young's modulus of elasticity.

2. Results and discussion

Using equations (1) – (5), we calculate the elastic parameters for graphite.

Table 2. Elastic parameters of graphite

Graphite	W_{aa}, J/m^2	W_{ac}, J/m^2	σ_{isa}, GPa	σ_{isc}, GPa	E_a, GPa	E_c, GPa
C (ρ = 2,26)	3,613	1,323	5,74	1,37	7,59	3,48
C (ρ = 1,75)	2,801	1,026	3,75	0,93	5,88	2,70
C (ρ = 1,65)	2,637	0,966	3,44	0,87	5,55	2,55

Graphite has an average value of T_m = 3970 K and γ_2 = 2.779 J/m^2. Internal stresses in graphite σ_{isc} lead to an increase in the interplanar distance (Fig. 5), which can be easily separated from the rest of the crystal with simple tape, turning it into graphene [34]. If we look at Fig. 4b, it can be seen that the friction process itself can be described as a process of elastoplastic deformation of the surface layer. Moreover, the nanolayer, which contains 3–5 atomic monolayers, behaves elastically and quickly collapses according to the Griffiths scheme, forming a layer like a solid lubricant. Energy W_{ac} is spent on this. Next, the mesolayer (or mesoscopic layer) enters into the friction process. In mesoscopics, it has been experimentally proven that plastic flow begins in a brittle material when it loses shear stability, which is fundamentally different from the previous case.

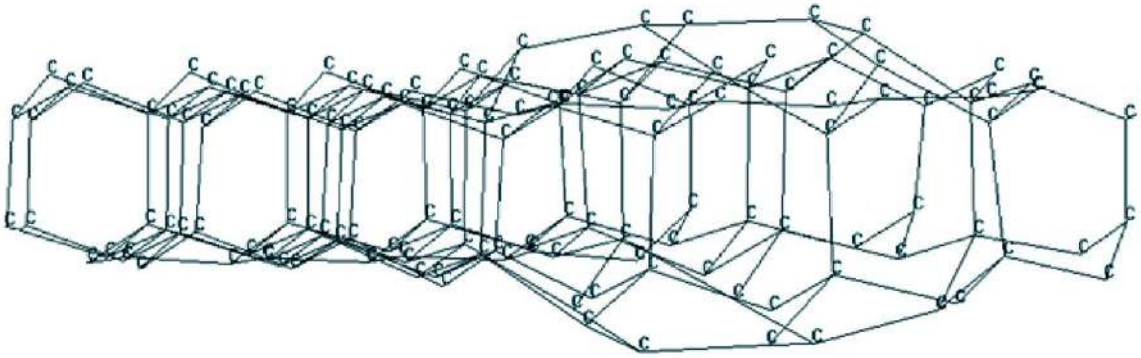

Fig. 5. Increasing the interplanar distance of the surface layer.

The characteristic length for mesoscopics is the phase coherence length hφ, which can vary within wide limits, but in mesoscopics it is always $h_\varphi \le 10^{-6}$ m = 1 micron.

As the upper graphite moves along the surface of the lower metal, a new surface of nanometer thickness is formed again. This means that friction performs an oscillatory motion (Fig. 6a). As soon as the speed exceeds a critical value and the formation of a nanolayer does not occur, friction begins to depend on speed. Layers R(I), R(II) and the bulk phase have different values of internal friction, which is proportional to the internal stresses ε_{isc} from the table. 2. When the graphite from above begins to move, a turbulent fragment appears due to friction (Fig. 6b).

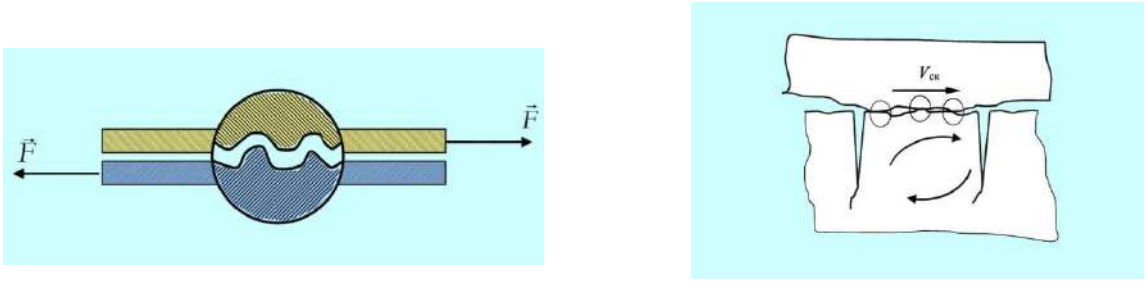

a) b)

Fig. 6. Oscillatory motion of friction during the formation of a new surface (a); diagram of the formation of a turbulent fragment (b)

This is manifested in the microstructure found on the surface of steel 20 [35] (Fig. 7a) and on our CrNiTiZrCu alloy [36] (Fig. 7b). There are many similarities between high-entropy alloys and metallic glasses [46]. A similar structure in Fig. 7 is typical for Bénard cells [37]. Bénard cells are the appearance of order in the form of convective cells in the form of cylindrical shafts or regular hexagonal figures in a layer of viscous liquid with a vertical temperature gradient. And the temperature gradient gradT ~ k, i.e. is proportional to the coefficient of internal and external friction, so friction is similar to a viscous fluid. So, the friction of graphite and layered materials on steel is similar to a viscous liquid, although there is another point of view [38]. In this paper, the distance dependence of non-contact friction on a graphite surface is studied using a quartz tuning fork with transverse vibration in the atmosphere. It is found that energy dissipation begins to increase when the distance is less than 2 nm, exhibiting a form of phonon dissipation. However, as the distance decreases further, the dissipation is different from the phonon dissipation and represents a huge friction energy dissipation peak, which is caused by the hysteretic behavior between the vibration of the surface atoms and the vibration of the tip. This work advances the understanding of the mechanism of energy dissipation in non-contact friction.

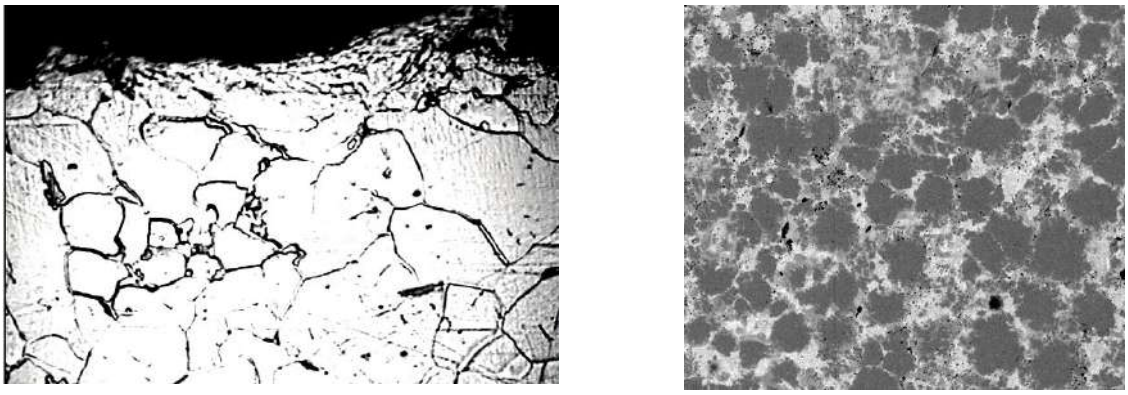

a) b)

Fig. 7. Friction surface at the moment of a turbulent fragment of a sample made of steel 20 [35] (a) and CrNiTiZrCu alloy [36] (b).

If the friction of graphite is considered similar to the friction of a viscous liquid, then from this approach it follows that friction depends on the speed of movement, has a structure similar to Benard cells, which means self-organization and friction synergism occurs. The fact that the friction of graphite cannot be explained using the usual Amonton law or on the basis of the hydrodynamic theory of lubrication is due to the fact that it is associated with the viscosity of the solution (viscous liquid), the theory of which has not yet been completed [39].

Using equations (1) - (5), we calculate the parameters for diamond [40].

Table 3. Diamond structure parameters

Diamond	(hkl)	Structure	R(I), nm	R(II), nm	γ, [41] J/m^2	γ, [42] J/m^2
C	100	Fd3m	0,29 (1)	2,61 (7)	9,100	9,300
	110		0,41 (1)	3,69 (7)	6,274	6,570
	111		0,68 (1)	6,12 (7)	5,270	5,400

From the table 1 it follows that the number of carbon monolayers in the R(I) layer of diamond is equal to one, like in graphene. The total thickness of the surface layer H = R(I) + R(II) is equal to: $H_{"100"}$ = 2.9 nm; $H_{"110"}$ = 4.1 nm; $H_{"111"}$ = 6.8 nm. The surface energy γ is significantly greater than all materials known in nature, which means its friction coefficient k ~ γ L (L is the length of the path traveled) should also be large. However (Fig. 3b), today it is believed that the low friction of diamond is due to the fact that its surface adsorbs air atoms (nitrogen, oxygen) and the surface turns into a solid lubricant similar to graphite [16]. Here we will present a different point of view. The elastic parameters of the surface layer of diamond are shown in table. 4.

Table 4. Properties of the surface layer of diamond

Diamond	(hkl)	$H_{(hkl)}$, nm	W_a, J/m^2	$\sigma_{(hkl)}$, GPa
C	100	2,9	11,83	58
	110	4,1	8,16	41
	111	6,8	6,85	29

The internal stresses $\sigma_{(hkl)}$ of metastable diamond are an order of magnitude greater than those of graphite and they are similar to the structure of silicon and germanium (Fig. 3a), in which covalent bonding is predominant. In

the bulk of C, Si, and Ge crystals, each atom forms four covalent bonds with its nearest neighbors located at the vertices of a regular tetrahedron. On the surface of the crystals, some of the bonds are broken, leading to its reconstruction [25]. For Si and Ge crystals, surface reconstruction and its models are presented in [43]. The Hanemann model consists of a chain of surface atoms that move up and down, but the bond length does not change compared to the bulk. In other words, the topology of the connections does not change, which has not been confirmed experimentally. Pendy's model, called the π-bonded atomic chain model. Here the communication topology changes completely: two six-bar rings of an idealized structure turn into five- and seven-bar rings. This model is recognized by many researchers, but it has not yet been confirmed experimentally.

In diamond, the bond between atoms is carried out by hybridized sp^3 orbitals. If we assume that diamond has two bonding electrons for each orbital in the crystalline volume, they are divided in half on the surface. This hybridization is associated with the excitation of electrons to an energetically higher state (Fig. 8). A structure consisting of three sp^2 orbitals and one p orbital may be more advantageous. This leads to a different distribution of electron density in space. In addition, sp^2 orbitals are localized almost exactly in the same plane. It follows that the surface layer of diamond turns into graphite during reconstruction. To prove this conclusion, consider the experimental results shown in Fig. 9. Here in Fig. 9a shows the photoluminescence of diamond, which clearly shows the difference between the glow of the surface layer and the bulk of the diamond.

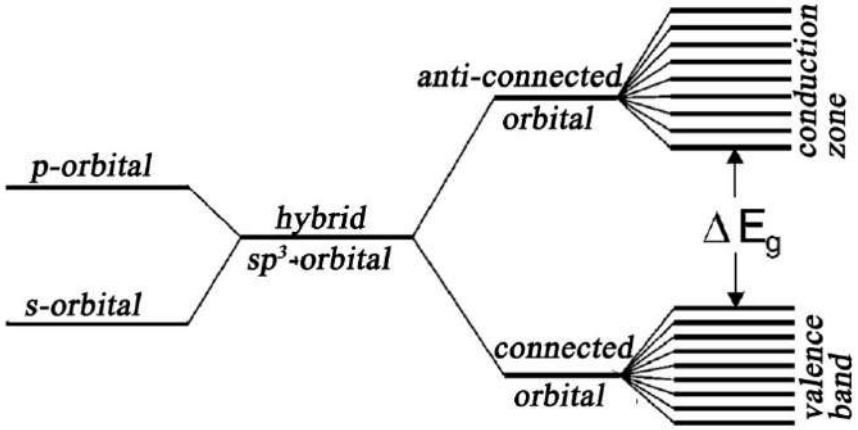

Fig. 8. Change in the energy of electronic states during hybridization of s- and p-orbitals [43]

Experimental Raman spectra of the surface layer of diamond are shown in Fig. 9b. In Fig. 9b D-peak (associated with carbons at the boundary of graphite crystallites) appears near 1350 cm^{-1}. The G-peak (associated with in-plane vibrations of graphite) is located near 1570 cm^{-1}. Both peaks are located against a luminescent background (Fig. 9b).

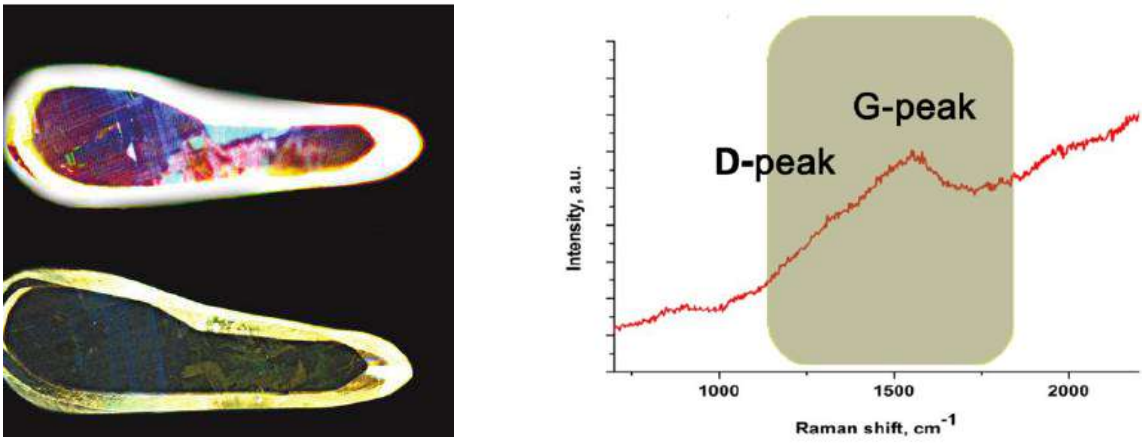

a) b)

Fig. 9. Photoluminescence of diamond samples [44], Raman spectra of the upper layer of diamonds [45]

Thus, the surface layer of metastable diamond, due to the reconstruction of its surface, becomes graphite and its friction coefficient is the same value (Fig. 3b). If you remove the surface layer of metastable diamond, i.e. turning it into a diamond, its friction coefficient will be $k \approx 0.6$ [16]. This means that our assumption about the formation of a surface layer of diamond can be considered proven.

Conclusions

Here we considered only two allotropic modifications of carbon - graphite (sp^2) and diamond (sp^3). There are other modifications of carbon: carbyne (sp); a series of fullerenes (sp^{2+x} or sp^{3-x}). The thickness of the surface layer of fullerene C_{96} is R(I) = 135 nm, which is three! order of magnitude higher than R(I) for diamond and graphite. Since friction, as shown above, is mainly determined by the surface layer, then for these modifications of carbon, determining the friction mechanism is a task for the near future.

References

[1] Frolov K.V. Modern tribology: Results and prospects. - M.: LKI Publishing House, 2008. - 480 p.
[2] Zhuravlev V.F. 500 years of history of the law of dry friction // Bulletin of MSTU im. N.E. Bauman. Ser. "Natural Sciences", 2014, No. 2. – P. 21-31.
[3] Shalygin M.G. Wear of sub-roughness of friction surfaces in a hydrogen-containing environment. – Dissertation of Doctor of Technical Sciences, Bryansk, 2017. – 235 p.
[4] Anthony K.-H. Thermodynamics of the friction process and Lagrangian formalism: contribution to the mesoscopic approach to the theory of plasticity // Physical mesomechanics, 2001, Vol. 4, No. 4. - P. 33-46.
[5] Yurov V.M., Guchenko S.A. Friction of high-entropy alloys and the thickness of their surface layer // Science of the XXI century, 2019, No. 8. - P. 14-16.
[6] Fedorov S.V. Assessment of the energy potential of mechanical (nano) friction quantum // Bulletin of science and education of the North-West of Russia, 2016, Vol. 2, No. 1. – P. 1-14.
[7] Baranov A.V., Vagner V.A., Tarasevich S.V. and others. Self-organization of tribosystems under boundary friction of metals // Polzunovsky Bulletin, 2009, No. 2. - P. 155-158.
[8] Pavelko G.F. Synergism and antagonism of anti-wear additives as a method of confirming the mechanism of their action // Friction and Wear, 2023, V. 44, No. 1. - P. 85-92.
[9] Grigoriev A.Ya., Myshkin N.K. Solid lubricants // Chemistry and Life, 2014, No. 1. – P. 34-42.
[10] Bolsunovskaya T.A., Efimochkin I.Yu., Sevostyanov N.V., Burkovskaya N.P. The influence of graphite grade as a solid lubricant on the tribological properties of a metal composite material // Proceedings of VIAM, 2018, No. 7 (67). – P. 69-77.
[11] GOST 17022–81. Graphite. Types, brands and general technical requirements. - M.: Standartinform, 2010. - 8 p.
[12] Belogorsky V.D. Antifriction graphite and its use in industry. - M.: Knowledge, 1974. - 154 p.
[13] Kazankapova M.K., Ermagambet B.T., Kasenov B.K., Nauryzbaeva A.T., Kasenova Zh.M., Kemelova B.A. Porous carbon materials based on carbon-mineral raw materials from Kazakhstan. Monograph. - Nur-Sultan: Institute of Coal Chemistry and Technology LLP, 2020. - 323 p.
[14] Kozhevnikov D.V., Grechishnikov V.A., Kirsanov S.V., Kokarev V.I., Skhirtladze A.G. Cutting tool. - M.: Mechanical Engineering, 2004. - 512 p.
[15] Vinokurov G.G., Sharin P.P., Popov O.N., Vinokurova S.G. Statistical description of the formation of microgeometry of the friction surface of a diamond drill // Friction and Wear, 2016, Vol. 37, No. 1. – P. 42-49.
[16] Handbook of Industrial Diamonds and Diamond Films / under general editorship M Prelas, G Popovici, L K Bigelow. - New York: CRC Press, 1997. - 1232 p.
[17] Bundy F.P., Bassett W.A., et al. The Pressure-Temperature Phase and Transformation Diagram for Carbon; Updated Through 1994 // Carbon, 1996, V. 34, No. 2. - P. 141-153.
[18] Sung J.C. and Lin J. Diamond nanotechnology. Syntheses and Applications. - Singapore, 2010. - 252 p.
[19] Gridin O.M., Teplova T.B., Gogotov A.A., Doronin M.A. Application of diamonds in industry and methods of their processing // Mining Information and Analytical Bulletin, 2013, No. 9 – P. 275-282.
[20] Khmelnitsky R.A., Talipov N.Kh., Chucheva G.V. Synthetic diamond for electronics and optics. - M.: IKAR Publishing House, 2017. - 228 p.
[21] [Stupnikov V.A., Bulychev B.M. High pressures in chemistry. diamond and diamond-like materials, technical and synthetic aspects. – M.: Moscow State University Publishing House, 2012. – 112 p.
[22] Kaminsky F.V., Voropaev S.A. Modern ideas about the genesis of diamond // Geochemistry, 2021, vol. 66, No. 11. - P. 993-1007.
[23] Kulakova I.I., Lisichkin G.V., Yakovlev R.Yu. Chemical modification of the surface of detonation nanodiamond. – M.: Moscow State University Publishing House, 2018. – 92 p.
[24] Kumar S, Nehra M, Kedia D, Dilbaghi N, Tankeshwar K, Kim K-H. Nanodiamonds: Emerging face of future nanotechnology // Carbon, 2019, Vol. 143. – P. 678-699.
[25] Oura K., Lifshits V.G., Saranin A.A., Zotov A.V., Katayama M. Introduction to surface physics. - M.: Science. 2006. - 490 p.
[26] Yurov V.M. Thickness of the surface layer of atomically smooth crystals // Physico-chemical aspects of studying clusters, nanostructures and nanomaterials. 2019. issue. 11. - P. 389-397.
[27] Yurov V.M., Goncharenko V.I., Oleshko V.S. Anisotropy of the surface layer of d-elements // Modern science-intensive technologies, 2021, No. 2. - P. 88–93.
[28] Yurov V., Zhangozin K. About the mechanism of mica splitting // Sciences of Europe, 2024, No. 133. – P. 97-104.

[29] Yurov V.M., Berdibekov A.T., Belgibekov N.A., Makhanov K.M. Friction of high-entropy coatings // Bulletin of KarU, 2021, No. 3. - P. 101-114.
[30] Yurov V., Zhangozin K. Surface layer thickness, defects and strength of graphite // The scientific heritage, 2023, No 128. – P. 20-27.
[31] Rekhviashvili S.Sh., Kishtikova E.V., Karmokova R.Yu. Towards the calculation of the Tolman constant // Letters to ZhTP, 2007, T. 33, Issue. 2. - P. 1–7.
[32] Yurov V.M., Goncharenko V.I., Oleshko V.S. Study of primary nanocracks in atomically smooth metals // Letters to ZhTP, 2023, vol. 49, issue. 8. - P. 35-38.
[33] Zimon A.D. Adhesion of films and coatings. - M.: Chemistry, 1977. – 352 p.
[34] Novoselov K.S. Graphene: materials of Flatland // Uspekhi Fizicheskikh Nauk, 2011, T. 181, No. 12. - P. 1299-1311.
[35] Kim V.A., Karimov Sh.A. Manifestation of physical mesomechanics during contact interaction, friction and wear // Scientific notes of KnAGTU, 2014, No. 11-1(18). – P. 5-9.
[36] Yurov V.M., Guchenko S.A., Makhanov K.M. High-entropy CrNiTiZrCu coatings and their properties // Trends in the development of science and education, 2021, No. 75, Part 1. – P. 107-114.
[37] Gershuni G.Z., Zhukhovnitsky E.M. Convective stability of an incompressible fluid. - M.: Nauka, 1972. - 232 p.
[38] Wang Ch., Liu H., Wang J., Han Y., Sun Z., Xu H., Liu H., Liu D. and Luo J. Non-contact friction energy dissipation via hysteretic behavior on a graphite surface // Nanoscale Adv., 2022, Vol. 4. – P. 4782-4788.
[39] Yurov V., Zhangozin K. Some questions of the theory of solution viscosity // German International Journal of Modern Science, 2023, No.71. – P. 34-41.
[40] Yurov V.M., Zhangozin K.N., Goncharenko V.I., Oleshko V.S. The thickness of the surface layer of diamonds // Endless Light in Science, 2024, No. 1. – P. 218-224.
[41] Harkins W. D. Energy Relations of surface of Solids // Journal Chem. Phys., 1942, V. 10. - P. 268-272.
[42] Nozhkina A.V., Kostikov V.I. Surface energy of diamond and graphite // Rock cutting and metalworking tools - equipment and technology for its manufacture and application: Sat. scientific tr. - Kyiv: INM im. V.M. Bakulya NAS of Ukraine, 2017, No. 20. - P. 161-167.
[43] Vladimirov G.G. Physics of the surface of solids. - St. Petersburg: Lan Publishing House, 2022. - 352 p.
[44] Klepikov I.V., Vasiliev E.A. Features of luminescence of the surface of diamond crystals // Ural Mineralogical School, 2022. – P. 78-80.
[45] Shashkov S.N. Raman microscopy of graphenes and other carbon structures // www.solinstruments.com
[46] Yurov V.M., Goncharenko V.I., Portnov V.S., Sha Mingun, Oleshko V.S., Rakhimova Zh.B., Rakhimov M.A., Rakhimova G.M., Maussymbayeva A.D. Anisotropy of the Surface Energy of Steel and Nickel Alloys in Aviation //Material and Mechanical Engineering Technology, №1, 2023 – C. 10-23

Information of the authors

Yurov Viktor Mikhailovich, c.ph.m.s, leading construction manager of LLP " TSC-Vostok"
e-mail: exciton@list.ru

Portnov Vassily Sergeevich, d.t.s., Abylkas Saginov Karaganda Technical University
e-mail: vs_portnov@mail.ru

Zhangozhin Kanat Nakoshevich, c.ph.m.s, associate professor, director of LLP "TSC-Vostok"
e-mail: 4kzh@mail.ru

Rakhimova Galiya Mukhamedievna, c.t.s., associate professor, Abylkas Saginov Karaganda Technical University
e-mail: g.rakhimova@kstu.kz

Rakhimova Zhanara, master of technical sciences, Abylkas Saginov Karaganda Technical University
e-mail: zhanara.rahimova.87@mail.ru